POLITECNICO
MILANO 1863

SCUOLA DI INGEGNERIA INDUSTRIALE
E DELL'INFORMAZIONE

Executive Summary of the Thesis

# Design of a MIMO SAR CubeSat Formation Flight Constellation for Maritime Surveillance

Laurea Magistrale in Space Engineering - Ingegneria Spaziale

**Author:** Lorcan Kelleher
**Advisor:** Prof. Andrea Monti-Guarnieri
**Co-advisor:** Dr. Davide Giudici
**Academic year:** 2021-2022

---

## 1. Introduction

Compact SAR formations operating in SIMO or MIMO mode are gaining interest in literature, with several flying demonstrations appearing in recent years. The interest stems from benefits including significant SNR gain and ambiguity suppression, enabling the design of a new generation of CubeSat-based SAR sensors. Additionally, multiple images can be generated of the same scene in slightly different times, enabling the identification and measures of moving targets (be them vehicles or sea currents), by along-track-interferometric approaches. These advantages are to be considered on top of the flexibility, robustness, and scalability common to distributed sensors formation. The all-weather-day-and-night capabilities of SAR imaging, make these formations valuable for several application in the field of emergency monitoring and security, specifically at sea.

This paper covers the design of a constellation of CubeSat formation flights for Synthetic Aperture Radar surveillance of maritime traffic, leveraging developments in MIMO distributed SAR systems to achieve system performance and a high revisit rate. The design is conducted using a set performance baseline for individual satellites and the constellation itself. These include an operational area of interest set as the Mediterranean Sea. The optimal formation size is investigated at a high level. Following this, the optimal constellation required to achieve the specified minimum performance is conceived using a multi-objective genetic algorithm (MOGA) and Walker pattern constellations.

The genetic algorithm focuses on system performance while also considering system cost; both monetarily and from a mission analysis point of view. Two separate configurations are considered in the formulation of the optimal solution; small swath and large swath strip map modes. Each configuration consists of a number of satellites in close formation flight in order to achieve the specified minimum performance. This investigation for a fixed pointing scan mode and a search mode, where the instrument can slew to the target. The performance of solutions output by the MOGA is examined across the target area. Finally, the lifetime of the constellation is investigated under several perturbations to assess constellation maintenance requirements.

# 2. MIMO SAR Formations

## 2.1. MIMO SAR Formation Benefits

Arising as a solution to the SAR paradox, MIMO SAR formations have many benefits over monolithic SAR systems. Firstly, an increase in the signal-to-noise ratio (SNR) of 60-92% of the number of satellites in the constellation squared is possible [1]. This is due to the combination of the antenna radiation patterns as well as the fact that all satellites in the constellation are actively transmitting and receiving. This performance is also better than the SIMO operating mode which improves the SNR by N, although it sampling tolerance must be more tightly controlled. A controller for the satellite spacing was considered to be out of the scope of this work. Considering the formation as a monolithic satellite with the pooled resources of antenna length and transmit/noise power from each of the individual satellites, the peak transmitted power required for a specific resolution looking at a target with a specific radar cross section for SIMO and MIMO operation respectively are:

$$\begin{cases} P_{T_{peak,SIMO}} = \dfrac{SNR_{min} P_{Noise} 4\pi^3 R^4}{G^2 \sigma \lambda^2 L^2}, & \text{(1a)} \\ P_{T_{peak,MIMO}} = \dfrac{SNR_{min} P_{Noise} 4\pi^3 R^4}{G^2 \sigma \lambda^2 L^2 N} & \text{(1b)} \end{cases}$$

The ability to suppress a number of azimuth ambiguities equal to the number of satellites in the formation minus 1, MIMO formations enable a lower choice of PRF versus simlar performing monolithic SAR systems. The trade-off to this is that the inter-satellite distance must be tighlty controlled to ensure said ambiguities are suppressed. Additionally, the benefits of robustness and flexibility due to distributed systems are a benefit which formation flights bring over monolithic SAR systems. All of this comes along with launch cost savings due to reduced spacecraft mass, and reduced service replacement costs due to smaller over spacecraft costs versus a larger monolithic system. This especially true when using CubeSats, which can use standardised COTS parts to reduce development and production costs.

These benefits of MIMO SAR formations have significant applications to a maritime monitoring constellation by providing a cost-effective high-resolution wide-swath imaging solution for vessel identification and tracking in a regional or global context.

## 2.2. Spacecraft CONOPS

### 2.2.1 Target Area and Targets

Before sizing a spacecraft for use in this design, the method of providing the maritime surveillance product first had to be established. With a significant rise in humanitarian, defense and illegal fishing activity in the Mediterranean in recent years, this area was chosen to be the target region of interest for this design. The target area was made by choosing a set of cities on the Mediterranean coastline as points and constructing a convex hull around them and is visible in figure 1 Most vessels involved in these types of activities are at minimum coaster size vessels[4], which was therefore decided as the primary target for the design process.

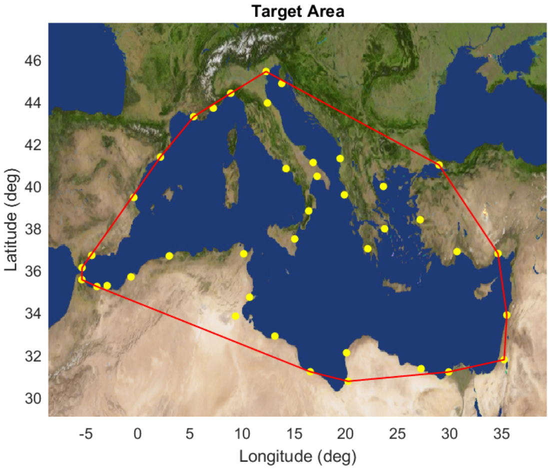

Figure 1: Target area

### 2.2.2 Configurations

Two main configurations were considered for the purposes of this investigation;

- a single-formation configuration (referred to as single-train or ST from here on)
- a wide-swath high resolution configuration (referred to as CubeSat MIMO Wide Swath or CMWS from here on)

For the sake of this design, all formations were assumed to fly in SAR trains as per Aguttes [2]. The CMWS configuration would be made up of a number of single-train formations flying in line, scanning different swaths of the same size. These swaths would then be stitched together to produce the final image. Each spacecraft was assumed to the same area in the along-track direction at the same time in this case as a simplification so that all instruments could be assumed to be looking at 0-Doppler.

### 2.2.3 Operating Modes

Two main operating modes were considered for the formation:

- Scan mode - where a fixed instrument pointing at a nominal elevation angle of 30 degrees was assumed for each formation
- Search mode - where the instrument was allowed to slew to the target.

Search mode was represented by allocating an equivalent swath to the formations equal to that which they could image if a continuous sweep was made from the minimum elevation angle all the way to the maximum. This was calculated to be approximately 417 km considering a spherical Earth geometry and equivalent Earth radius of 6371 km.

Search mode represents how current SAR solutions operate, where an area is searched for a vessel given last-known location information or supplementary AIS data. In a true maritime surveillance solution, this may not be available and so the scan mode is what would most likely be used. This was therefore assumed to be the nominal mode for the constellation operations.

## 2.3. Spacecraft System Requirements

Though some missions are in development such as the SRI-CIRES mission by NASA and SRI International, none have flown yet. This means that a set of spacecraft performances must be estimated from literature and existing services for use in the constellation design. Some of the most well-known SAR missions in the Copernicus portfolio are NOVASAR-S, ICEYE, Capella X-SAR and Sentinel-1.

As such, these spacecraft were used to guide the sizing of the spacecraft used for this design. To account for the difference in form factor between commercial solutions and the hypothetical CubeSat in use, a significant margin of 20% was applied to relevant design numbers to make performance estimates. Having surveyed these active spacecraft and applied the relevant margins, the performance of the theoretical CubeSat used in the design and its SAR instrument were defined and are summarised in table 1. Radar clutter due to ocean and weather conditions was accounted for in the system losses [7], as this was not simulated in the optimisation.

| Parameter | Value |
|---|---|
| **Size** | 16U |
| **Orbit Altitude** | 500 km |
| **Elevation Angles** | 15-45$^o$ |
| **Orbit Altitude** | 500 km |
| **Max Peak Power** | 400 km |
| **Max Duty Cycle** | 15% |
| **Max Bandwidth** | 100 MHz |
| **Single-Train Swath Size** | 30 km |
| **Ground Resolution** | 5 X 5 m |
| **Carrier Frequency** | 9.45-9.75 GHz |
| **Antenna Length** | 2.2 m |
| **Antenna Height** | 0.5 m |
| **System Losses** | 12 dB |
| **Required SNR** | 8-9 dB |

Table 1: Individual CubeSat and instrument performance summarised

## 2.4. MIMO Formation Sizing

Investigating the minimum formation required to meet the requirements set out in section 2.3, the worst case scenario for the radar sensing was assumed. This occurred at the highest frequency, targeting a vessel with the smallest RCS in the range of interest (defined in section 2.2) and at the edge of the imaged swath with the instrument pointed at the highest elevation angle. A formation size of 3 was found to satisfy the minimum requirements for the single-train case. A formation of 2 satellites would not be feasible due to destructive interference between instruments as per Giudici et. al [1]. To create the CMWS configuration, it was decided that 5 formations would fly in-line to produce a 150km-wide swath. The peak power required per formation size can be seen in figure 2. Considering the size of the swath and a basic correct reception requirement, the optimal duty cycle was found to be 10.8%, producing an average power of 42.8892 W, similar to current offerings by Capella and NOVASAR.

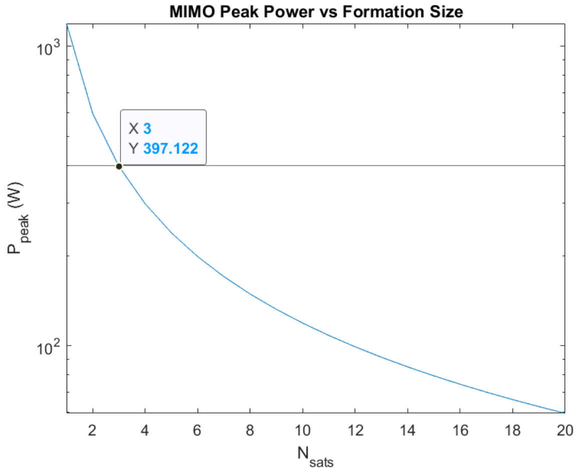

Figure 2: Peak power vs formation size

Analysing the required bandwidth across the swath to produce the required resolution, the maximum bandwidth chosen was found to be insufficient for the chosen resolution at the minimum pointing angle (from the boresight to the nearside of the imaged swath). This means that either a lower resolution would have to be accepted in these regions of the image, or the maximum possible bandwidth would need to be increased.

# 3. Constellation Design

## 3.1. Walker Constellations

To reduce the size of the search space for the genetic algorithm while also simplifying the design problem, it was decided to explore Walker Delta and Star patterns [6] as solutions. Walker pattern constellations consist of P orbital planes, equally separated in right ascension with the same orbital inclination. T satellites are evenly distributed among the orbital planes, and satellites in each plane are phased with a relative phasing of one pattern unit 2:

$$PU = \frac{360 * F}{T} \tag{2}$$

It is also clear here that to avoid self-collisions, T must not equal F as there would be no relative phasing between planes. Walker Delta patterns usually have planar inclinations of $30^o$ to $60^o$ but in any case less than 90 $^o$ with all satellites usually on circular orbits. Walker Star patterns consist of polar orbits (i=$90^o$), also usually with circular orbit shapes. The circular orbit assumption was taken for this design. Usually, these patterns are used for global coverage applications while streets-of-coverage patterns are used for regional design problems like this one. However, Walker Delta and Star patterns have been used in literature to cover large regions [5], similar to the one used in this problem. They are also simpler and easier to design than some other constellations patterns. While this decision may result in designs which use too few planes for sufficient global coverage and too many planes for a set regional coverage, its benefits in simplifying the design problem and reducing the search space were decided to exceed its drawbacks for this application.

## 3.2. Constellation Performance Requirements

The target area was split into a grid with a coarse density for the design process, which was refined to a tighter mesh for performance analysis. For the maritime surveillance application, the constellation performance metrics were defined as:

1. Average point leakage time (s)
2. Area coverage (%)
3. Leak Time Deviation (s)
4. Number of formations used
5. Number of orbital planes
6. Difference in inclination from launcher minimum (rad)

Point leakage time was defined as the time taken for a point in the grid to be identified. This best reflects the revisit performance of the constellation. This and the area coverage were deemed to be the most important performance parameters for maritime surveillance applications, as leak time deviation mainly indicates coverage uniformity. The latter 3 metrics are measures of cost in both delta-v for manoeuvring to setup or replace spacecraft and monetarily in manufacturing or service procurement. Surveying the same existing services explored in the literature review of section 2.3 and considering the system requirements set in that section, the constellation performance requirements were set as:

- Average point leakage time $<$ 6 hours
- Area coverage $>$ 85%

- Maximum number of launches for deployment = 5

The assumption was made that a vessel being tracked continued to travel in a straight line at the same speed during the entire simulation. The heading chosen could be any, and so between positive identifications by any spacecraft in the constellation, it was assumed that a circular area of radius $v_{vessel} * t$ existed in which the vessel could be located at any point. This created a bubble of maximum positional uncertainty, the size of which was limited by the average speed for the vessel class. In this case the maximum tracking positional uncertainty ($\Delta_{pos}$)was set to be $+/-$ 166km, given the average speed of 12-14 knots for the coaster vessel class.

## 3.3. Working Point

To establish a baseline solution for comparison with the MOGA outputs, a set of working point solutions for scan mode was generated by manual iteration which achieved the required constellation grid performance. This is summarised in table 2.

| Parameter | ST | CMWS |
|---|---|---|
| **P** | 55 | 11 |
| **Inclination** | 0.7662 rads | 0.7662 |
| **Formations** | 55 | 11 |
| **F** | 1 | 1 |
| $\boldsymbol{\Omega_0}$ | 4.9334 rads | 4.9334 rads |
| **Mean** $t_{leak}$ | 5.63 hrs | 5.614 hrs |
| $A_{cov}$ | 90.938% | 89.704% |

Table 2: Working point configurations and performances

# 4. Multi-Objective Genetic Algorithm

A multi-objective genetic algorithm (MOGA) was used to optimise the problem. MOGAs used Darwin's theory of natural selection and are useful when optimising problems with large search spaces and multiple variables. These algorithms work by evaluating a set of fitness functions defined by the uses, and defining a set of values for some variables (which the algorithm controls) for a number of individual points. This process tends to produce Pareto fronts; a visualisation of the best possible solutions given a set of fitness functions. In this case, the fitness functions were set as the constellation performance metrics from section 3.2. A population of 200 and 100 generations was used for the optimisation.

## 4.1. Setup and Constraints

The minimum inclination for any orbital plane was set by the instrument off-nadir geometry and the highest point of the target area. This value was set such that the far edge of the instrument beamwidth could always acquire the highest point in terms of latitude in the target area. The MOGA was given control over the number of planes, formations used, orbit inclination, phasing constant and right ascension of the first orbital plane. As formations and not satellites were considered, each formation in the single-train case represents 3 satellites, while in the CMWS case it represents 5. Considering the Walker patterns used and thus the restrictions imposed in section 3.1, the optimisation problem could be summarised as per equation 4.1.

$$\begin{cases} \min(P, T, (\Delta i), \mathrm{t}_{leak}, \mathrm{std}(t_{leak}), \frac{1}{A_{cov}}) & (3) \\ P \in [1,\ \mathrm{T}], & (4) \\ i \in [i_{min},\ 90^o], & (5) \\ F \in [1,\ \mathrm{T\text{-}1}], & (6) \\ T \in [1,\ 60], & (7) \\ \Omega_0 \in [1,\ 360^o] & (8) \end{cases}$$

Considering these constraints, this problem was defined as a nonlinear mixed-integer problem with a large search space. A computation time in the order of hours was expected. Each orbit was propagated for 24 hours with a time step of 60 seconds for the optimisation algorithm. Ode113 was used to propagate the orbits because along with a real instrument geometry, a desire was expressed not to sacrifice the realistic depiction of performance too much for computational efficiency.

## 4.2. Algorithm

The MOGA algorithm is summarised in 1. Gamultiobj in MATLAB's optimisation toolbox was used for this task.

Algorithm 1 MOGA evaluation algorithm

```
for Each Generation do
    for each individual in generation do
        Setup Constellation
        Create Targets
        for each formation do
            check if instrument swath in tgt area
            if yes then
                for each time step swath in tgt area do
                    Make polygon from max and min latitude of instrument reach
                    if point in polygon then
                        Add time of acquisition to grid point list
                    end if
                end for
            end if
            Calculate Performance
        end for
        Evaluate Fitness
    end for
    if Requirements met then
        end
    else
        Mutate, crossover, next generation
    end if
end for
```

## 5. Results and Discussion

| **Variable** | **ST MOGA** | **CMWS MOGA** | **Search** | **ST WP** | **CMWS WP** |
|---|---|---|---|---|---|
| **P** | 60 | 1 | 1 | 55 | 11 |
| **i (rads)** | 0.7447 | 0.75403 | 0.7603 | 0.7662 | 0.7662 |
| $N_{Forms}$ | 60 | 12 | 12 | 55 | 11 |
| **F** | 1 | 1 | 1 | 1 | 1 |
| $\Omega_0$ **(rads)** | 6.2832 | 5.7637 | 0.23904 | 4.9334 | 4.9334 |
| **Mean** $t_{leak}$ **(hrs)** | 4.8733 | 5.359 | 2.3658 | 5.63 | 5.614 |
| $A_{cov}$(%) | 91.119 | 88.3079 | 91.68 | 90.938 | 89.704 |

Table 3: MOGA configurations and performances

Table 3 shows the best MOGA individuals compared to the working point (WP) solutions, where i represents orbital plane inclination and $N_{forms}$ the number of formations. For the tracking simulation, a pleasure craft ported in Malta was geolocated using an AIS database[3] and its parameters modelled in the simulation. It was assumed to be on a straight East-West course starting from a random point in the East of the target area, travelling at half of its average speed to account for pleasure stops and un-modelled winds etc.

| | **ST** | **CMWS** | **Search** |
|---|---|---|---|
| $\Delta_{pos}$ **(km)** | 215.916 | 120.237 | 89.546 |

Table 4: MOGA constellations tracking performance

Performance was simulated with a tighter grid meshing approximately 10% that used in the MOGA design to give a better visualisation of the performance and a finer time step of 5 seconds. This resulted in improved performance across the target area for each constellation as some passes through the area which may have been skipped due to the larger time step were not omitted. It is possible this resulted in some marginal constellation combinations being omitted. The benefits of CMWS configuration over single-train clearly manifested themselves in tracking performance, most important for maritime surveillance applications. However, it was also observed that in general operating a CMWS configuration allowed to obtain the same or better performance with fewer satellites as shown in the combined Pareto plots in figures 3 and 4 respectively. A maximum number of launches of 5 was considered with a launch capacity of 36 satellites per launcher. Given the configurations considered this is why CMWS and search mode plots stop at 12 formations.

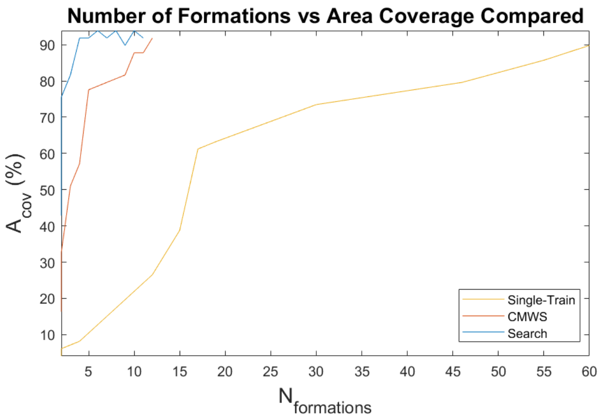

Figure 3: Pareto plots of number of formations vs area coverage

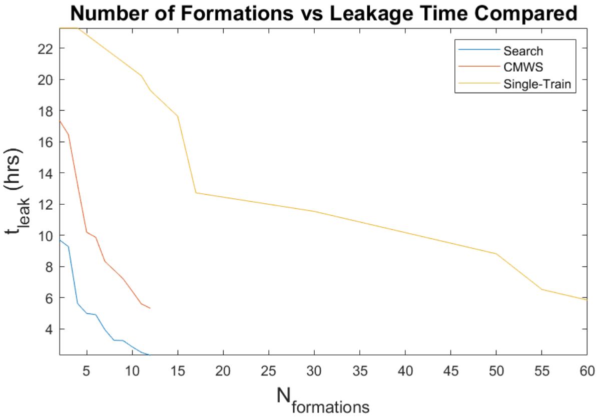

Figure 4: Pareto plots of number of formations vs leakage time

The search mode performed best as anticipated, but the requirement of supplementary information may make it an unfavourable operating mode for this application. The optimal constellation design as such depends on the potential operator, but the best performance for these objectives would be achieved by the CMWS best individual operating in search mode.

The MOGA produced solutions which tended towards lower inclinations. This was expected due to the minimisation of the inclination difference as an objective, along with the fact that the target area was wider than it was tall, so more points would be covered by a more horizontal path through it achieving better performance.

Fewer planes were also preferred in almost all cases, due to this being a minimisation term but this was also likely impacted by the Walker pattern usage and the dimensions of the target area. Plane combinations of 2 or 3 would spread the planes such that a solution with more satellites in a single plane would achieve better leakage time performance.

The chosen solution performed comparably to current competing solutions in terms of revisit time, with a much improved swath size.

| **Service** | **Satellites in Constellation** | **Point Revisit Time (hrs)** | **Swath Width (km)** |
|---|---|---|---|
| NovaSAR-S | 3 | 14.4 | 20 |
| Sentinel-1 | 2 | 48 | 80 |
| Capella | 36 | $\leq 1$ | 5 |
| ICEYE | 18 | 20 | 30 |
| CMWS Search | 180 | 2.3658 | 150 |

Table 5: Solution performance compared to competing services

Assuming each satellite had a cold-gas thruster and 25m/s delta-v available, the lifetime of each constellation was analysed. This could be done as it was assumed each formation manoeuvred at the same time in the same way, and experienced the same orbital perturbation effects over their lifetime. Additionally, it was assumed that insertion was performed by the launcher upper stage or a last-mile delivery vehicle. A manoeuvre was given if a deviation of $3\sigma$ from the mean orbital elements was observed. This resulted in an operational lifetime of approximately 3 months for each formation and for all constellation combinations, with an orbit decay time of 7 months. It was recommended to change to an electrical propulsion solution to allow for 10 times the operational lifetime, similar to competitors which fly for 1-3 years. A trade-off study examining an increased orbit height versus operational lifetime gain would be a worthwhile extension of this work.

## 6. Conclusions

A set of constellations were produced for both configurations and operating modes which demonstrated the benefits of using MIMO SAR formations in constellations for maritime surveillance purposes. The CMWS mode performed better in maritime tracking applications, while the single-train mode compensated for its smaller swath with more orbital planes to achieve similar revisit performance. The unseen benefit of CMWS is also that more ships could theoretically be tracked simultaneously than single-train. The search mode performed best as expected, but it may be a sub-optimal solution due to the requirement of supplementary information to function. Regardless, the number of formations used in search mode could be reduced and the minimal performance could still be achieved, making it the most efficient solution.

The MOGA results provided an improvement over the manual iterations, however it was clear that the approach taken to the problem was not ideal from the point of view of computational efficiency especially.

The usage of Walker Delta and Star patterns along with the simulation period of 24 hours and the 60 second time step my have been sub-optimal, mainly due to the number of single-plane solutions generated. A regional coverage pattern and a larger simulation period may address this issue but must be examined in future works.

An effort was made to generate results which gave a more realistic insight into the performance of such a constellation using these MIMO formations. This was of course at the expense of compute power and thus algorithm convergence. Using a population of 200 and 100 generations the algorithm did not converge to a solution due to the 1e-6 tolerance, after compute times of up to 45 hours. This could be improved with semi-analytical methods, which also provide the benefit of more intelligible relations showing the impact of certain parameters on constellation performance without the need of any simulation. This is something which could be improved with future work.

Finally, satellites in the constellation should utilise electrical propulsion to achieve an operational life on par with the competing solutions from industry.

## 7. Acknowledgements

I would like to thank Professor Monti-Guarnieri and Doctor Giudici for their guidance and patience throughout the production of this work and Professor Tebaldini for connecting me with incredible opportunity. I would also like to thank Professor Gonzalo-Gomez for his availability and guidance on short notice. To all of the staff at Politecnico di Milano for their hard work each day to create the environment in which this work could be safely and successfully completed. I would like to dedicate this work to m family, without whom none of this would have been possible.

## References

[1] Davide Giudici, Pietro Guccione, Marco Manzoni, Andrea Monti Guarnieri, and Fabio Rocca. Compact and free-floating satellite mimo sar formations. *IEEE Transactions on Geoscience and Remote Sensing*, 60:1–12, 2022.

[2] Aguttes. J-P. Formations orientées le long du trajet de satellites sar, 6 2003.

[3] MarineTraffic.com. Marinetraffic: Global ship tracking intelligence | ais marine traffic.

[4] Nathan A. Miller, Aaron Roan, Timothy Hochberg, John Amos, and David A. Kroodsma. Identifying global patterns of transshipment behavior. *Frontiers in Marine Science*, 5, 7 2018.

[5] Yuri Ulybyshev. Satellite constellation design for complex coverage. *Journal of Spacecraft and Rockets*, 45:843–849, 2008.

[6] J. G. Walker. Satellite constellations. *Journal of the British Interplanetary Society*, 37:559, 12 1984.

[7] Tao Wu, Zhensen Wu, Jiaji Wu, Gwanggil Jeon, and Liwen Ma. Features of x-band radar backscattering simulation based on the ocean environmental parameters in china offshore seas. *Sensors (Switzerland)*, 18, 8 2018.